

Highly Stable Hexacoordinated Nonoxidovanadium(IV) Complexes of Sterically Constrained Ligands: Syntheses, Structure, and Study of Antiproliferative and Insulin Mimetic Activity

Subhashree P. Dash,[†] Sagarika Pasayat,[†] Saswati Bhakat,[†] Satabdi Roy,[†] Rupam Dinda,^{*,†} Edward R. T. Tiekink,[§] Subhadip Mukhopadhyay,^{||} Sujit K. Bhutia,^{||} Manasi R. Hardikar,[⊥] Bimba N. Joshi,[⊥] Yogesh P. Patil,[‡] and M. Nethaji[‡]

[†]Department of Chemistry, National Institute of Technology, Rourkela 769008, Odisha, India

[§]Department of Chemistry, University of Malaya, 50603 Kuala Lumpur, Malaysia

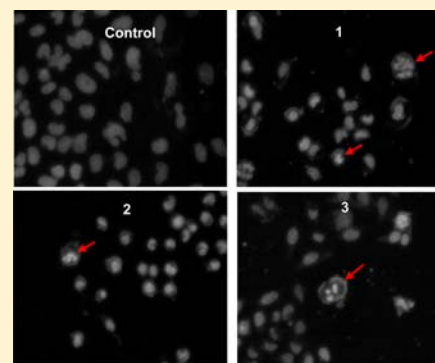
^{||}Department of Life Science, National Institute of Technology, Rourkela 769008, Odisha, India

[⊥]Biometry and Nutrition Group, Agharkar Research Institute, G.G. Agrakar Road, Pune 411004

[‡]Department of Inorganic and Physical Chemistry, Indian Institute of Science, Bangalore 560012, India

S Supporting Information

ABSTRACT: Three highly stable, hexacoordinated nonoxidovanadium(IV), $V^{IV}(L)_2$, complexes (1–3) have been isolated and structurally characterized with tridentate arylhydrazonates containing ONO donor atoms. All the complexes are stable in the open air in the solid state as well as in solution, a phenomenon rarely observed in nonoxidovanadium(IV) complexes. The complexes have good solubility in organic solvents, permitting electrochemical and various spectroscopic investigations. The existence of nonoxidovanadium(IV) complexes was confirmed by elemental analysis, ESI mass spectroscopy, cyclic voltammetry, EPR, and magnetic susceptibility measurements. X-ray crystallography showed the N_3O_3 donor set to define a trigonal prismatic geometry in each case. All the complexes show in vitro insulin mimetic activity against insulin responsive L6 myoblast cells, with complex 3 being the most potent, which is comparable to insulin at the complex concentration of $4 \mu M$, while the others have moderate insulin mimetic activity. In addition, the in vitro antiproliferative activity of complexes 1–3 against the HeLa cell line was assayed. The cytotoxicity of the complexes is affected by the various functional groups attached to the bezoylhydrazone derivative and 2 showed considerable antiproliferative activity compared to the most commonly used chemotherapeutic drugs.



INTRODUCTION

Vanadium attracts increasing interest in biochemistry.^{1,2} Of the numerous reported effects of vanadium on organisms, its stimulatory effect on the growth of algae and plants,³ the inhibitory action of vanadate(V) on Na, K-ATPase,⁴ the presence of vanadium at the active site of certain enzymes, including haloperoxidases in sea algae and lichens⁵ and some nitrogenases in nitrogen-fixing *Azotobacter*⁶ are especially worth mentioning. Moreover, inorganic vanadyl and vanadate, as well as some vanadium(IV) and (V) complexes, are potent insulin mimics and as such may find use as alternatives to insulin in the treatment of diabetes.⁷ The discovery of the in vivo insulin mimesis per os of oxidovanadates(V),⁸ the oxidovanadium(IV) precursor, vanadyl sulfate,⁹ and the much more potent bis(maltolato)-oxidovanadium(IV) (BMOV)¹⁰ stimulates the search for vanadium complexes which may have application in the treatment of type II diabetes.^{11,12} Different approaches have been attempted to develop more potent and orally active vanadium-containing insulin-enhancing agents.¹³ Although the said complexes have shown pharmacological advantages

compared to the uncomplexed $VOSO_4$, further improvement in ligand design is needed, focusing on identifying new vanadium complexes with increased potency and decreased toxicity.¹⁴

In the past few years, new metal complexes have been identified as a very promising class of anticancer active compounds.^{15–22} Some vanadium complexes, particularly, peroxidovanadates(V) and bis(cyclopentadienyl)vanadium(IV) complexes,²³ have been found to possess antitumor activity. Recently, some new types of oxidovanadium(IV) complexes, mono(phenanthroline)oxidovanadium(IV) $[VO(phen)-(H_2O)_2]^{2+}$ ²⁴ and bis(1,10-phenanthroline)sulfatooxidovanadium(IV) $[VO(SO_4)(phen)_2]$,²⁵ were reported to exhibit potent antitumor activity against the human nasopharyngeal carcinoma-KB cell line and the clonogenic NALM-6 cell line, respectively. Dong et al. have reported the cytotoxic activity of some bis(phenanthroline)oxidovanadium(IV) complexes

Received: July 24, 2013

Published: December 4, 2013

against the human leukemic NALM-6 cell line.²⁵ Noletto and co-workers described the cytotoxic activity of some GALMAN-A:VO²⁺/VO³⁺ and GALMAN-B:VO²⁺/VO³⁺ complexes against HeLa cells.²⁶ Very recently, Sasmal et al. have reported the photocytotoxicity of the oxidovanadium(IV) complex [VO(L)-(B)]Cl₂, where L is bis(2-benzimidazolylmethyl)amine and B is dipyrrodo[3,2-a:2',3'-c]phenazine against the adenocarcinoma A549 cell line.²⁷

However, in contrast to the well-known vanadium(IV)/(V) complexes containing VO²⁺ or VO³⁺ units,²⁸ only very few octahedral nonoxido V^{IV} and V^V complexes, the so-called “bare” complexes, have been isolated and structurally characterized.²⁹ Amavadin,³⁰ a compound isolated from the mushroom *Amanita muscaria*, has been shown to contain an octacoordinated V⁴⁺ ion³¹ without oxido ligands, but such nonoxido vanadium species are still scarce.²⁹

On the other hand, hydrazones, –NH–N=CRR' (R and R' = H, alkyl, aryl), are versatile ligands due to their applications in the field of analytical³² and medicinal chemistry.³³ Hydrazone moieties are the most important pharmacophoric cores of several anticancer, antiinflammatory, antinociceptive, and antiplatelet drugs.³⁴ In the context of the present study, it is relevant to mention that although the chemistry of oxidovanadium(IV)-aroylhydrazone complexes is well developed,³⁵ far less information is available for model nonoxido complexes,^{29a,p} particularly concerning their biological properties.

We have been studying the chemistry of oxido–metal complexes, including those of vanadium in O–N containing donor environments³⁶ along with electro generation of mixed-valence divanadium(IV,V) complexes,^{36a,b} and herein we report the syntheses and X-ray crystal structures of three nonoxidovanadium(IV) complexes containing aroylhydrazones along with special reference to their insulin mimetic and antiproliferative activities. These nonoxido V^{IV} complexes were fully characterized by various physicochemical techniques like IR, EPR, ESI mass, electronic spectroscopy, magnetic susceptibility studies, and electrochemical investigations.

EXPERIMENTAL SECTION

General Methods and Materials. All chemicals were purchased from commercial sources and used without further purification. [VO(acac)₂] was prepared as described in the literature.³⁷ Reagent grade solvents were dried and distilled prior to use. The L6 myoblast cell line derived from a rat was procured from NCCS, Pune, India. Penicillin, streptomycin, DMEM, fetal bovine serum, and insulin were purchased from Invitrogen (San Diego, CA), and the glucose estimation kit was purchased from Randox. MTT (3-[4,5-dimethylthiazol-2-yl]-2,5-diphenyltetrazolium) and DAPI (4',6-diamidino-2-phenylindole dihydrochloride) were purchased from Sigma Aldrich (St. Louis, MO). Minimal essential medium (MEM) was purchased from Gibco, India. Elemental analyses were performed on a Vario ELcube CHNS Elemental analyzer. IR spectra were recorded on a Perkin-Elmer Spectrum RXI spectrophotometer. ¹H and ¹³C NMR spectra were recorded on a Bruker Ultrashield 400 MHz spectrometer using SiMe₄ as an internal standard. Electronic spectra were recorded on a Lambda25, PerkinElmer spectrophotometer. Mass spectra were obtained on a SQ-300 MS instrument operating in ESI mode. DC magnetic susceptibility measurements were carried out on a Vibrating Sample magnetometer, PPMS (Physical Property Measurement System, Quantum Design, U.S.A.) in the

temperature range from 2–300 K with an applied field of 1 T. Electrochemical data were collected using a PAR electrochemical analyzer and a PC-controlled potentiostat/galvanostat (PAR 273A) at 298 K in a dry nitrogen atmosphere. Cyclic voltammetry experiments were carried out with Pt working and auxiliary electrodes, Ag/AgCl as the reference electrode, and TEAP as the supporting electrolyte. X-band EPR measurements were performed on a JEOL JES-FA 200 and Bruker EMX EPR Spectrometer.

Synthesis of Ligands (H₂L^{1–3}). Schiff base ligands, anthranilylhydrazone of 2-hydroxy-1-acetonaphthone (H₂L¹), salicylhydrazone of 2-hydroxy-1-acetonaphthone (H₂L²), and benzoylhydrazone of 2-hydroxy-1-acetonaphthone (H₂L³) were prepared by the condensation of 2-hydroxy-1-acetonaphthone and the respective acidhydrazide in equimolar ratio in ethanol by a standard procedure.³⁸ The resulting white compounds were filtered, washed with ethanol, and dried over fused CaCl₂. Elemental analysis results, NMR (¹H and ¹³C), and IR data for all of these verified their preparation.

H₂L¹. Yield: 64%. Anal. Calcd. for C₁₉H₁₇N₃O₂: C, 71.46; H, 5.36; N, 13.16. Found: C, 71.48; H, 5.37; N, 13.14. IR (KBr pellet, cm⁻¹): 3473 ν(O–H); 3410 ν(NH₂)_s; 3329 ν(NH₂)_{as}; 3221 ν(NH); 1663 ν(C=O); 1553 ν(C=N). ¹H NMR (400 MHz, DMSO-*d*₆): δ 10.35 (s, 1H, naphthyl–OH), 9.17 (s, 1H, NH), 7.91–6.23 (m, 10H, aromatic), 6.05 (s, 2H, NH₂), 2.35 (s, 3H, CH₃). ¹³C NMR (100 MHz, DMSO-*d*₆): δ 153.98 (CO–N), 152.47 (N=C(Me)), 152.36–113.59 (16C, aromatic), 24.15 (–CH₃).

H₂L². Yield: 60%. Anal. Calcd. for C₁₉H₁₆N₂O₃: C, 71.24; H, 5.03; N, 8.74. Found: C, 71.28; H, 5.01; N, 8.71. IR (KBr pellet, cm⁻¹): 3542 ν(O–H); 3113 ν(N–H); 1661 ν(C=O); 1555 ν(C=N). ¹H NMR (400 MHz, DMSO-*d*₆): δ 10.84 (s, 1H, phenyl–OH), 10.37 (s, 1H, NH), 10.21 (s, 1H, naphthyl–OH), 7.94–6.69 (m, 10H, aromatic), 2.32 (s, 3H, CH₃). ¹³C NMR (100 MHz, DMSO-*d*₆): δ 161.19 (CO–N), 155.89 (N=C(Me)), 152.50–114.52 (16C, aromatic), 24.09 (–CH₃).

H₂L³. Yield: 58%. Anal. Calcd. for C₁₉H₁₆N₂O₂: C, 74.98; H, 5.29; N, 9.20. Found: C, 74.96; H, 5.32; N, 9.21. IR (KBr pellet, cm⁻¹): 3337 ν(O–H); 3071 ν(N–H); 1659 ν(C=O); 1573 ν(C=N). ¹H NMR (400 MHz, DMSO-*d*₆): δ 10.31 (s, 1H, naphthyl–OH), 9.55 (s, 1H, NH), 7.91–7.27 (m, 11H, aromatic), 2.34 (s, 3H, CH₃). ¹³C NMR (100 MHz, DMSO-*d*₆): δ 153.71 (CO–N), 152.63 (N=C(Me)), 152.12–113.74 (16C, aromatic), 24.30 (–CH₃).

Synthesis of Complexes [V^{IV}(L^{1–3})₂] (1–3). A general synthetic procedure taking [VO(acac)₂] as representative metal precursor is described below:

[VO(acac)₂] (0.5 mmol) was added to a hot solution of the appropriate ligand H₂L^{1–3} (1.0 mmol) in EtOH (20 mL), and the color changed instantly to greenish black. After 3 h of stirring, red (1, 2) and dark green (3) crystals were obtained from the reaction mixture, which were filtered off, washed thoroughly with ethanol, and dried. Some crystals were of diffraction quality and were used directly for X-ray structure determination using single crystal X-ray diffractometer.

[V^{IV}(L¹)₂] (1). Yield: 66%. Anal. Calcd. for C₃₈H₃₀N₆O₄V: C, 66.57; H, 4.41; N, 12.26. Found: C, 66.55; H, 4.37; N, 12.29. IR (KBr pellet, cm⁻¹): 3298 ν(NH₂)_s; 3043 ν(NH₂)_{as}; 1589 ν(C=N); 1256 ν(C–O)_{enolic}; 1048 ν(N–N). ESI-MS (CH₂Cl₂): *m/z* 708.49 (53%, [M + Na]⁺); ESI-MS (CH₃CN + CH₂Cl₂) (19:1): *m/z* 708.12 (100%, [M + Na]⁺); ESI-MS (MeOH + DMF) (19:1): *m/z* 708.21 (100%, [M + Na]⁺).

Scheme 1. Schematic Diagram of Various Pathways through Which the Hexacoordinated $V^{IV}(L)_2$ Nonoxidovanadium(IV) Complexes Were Synthesized

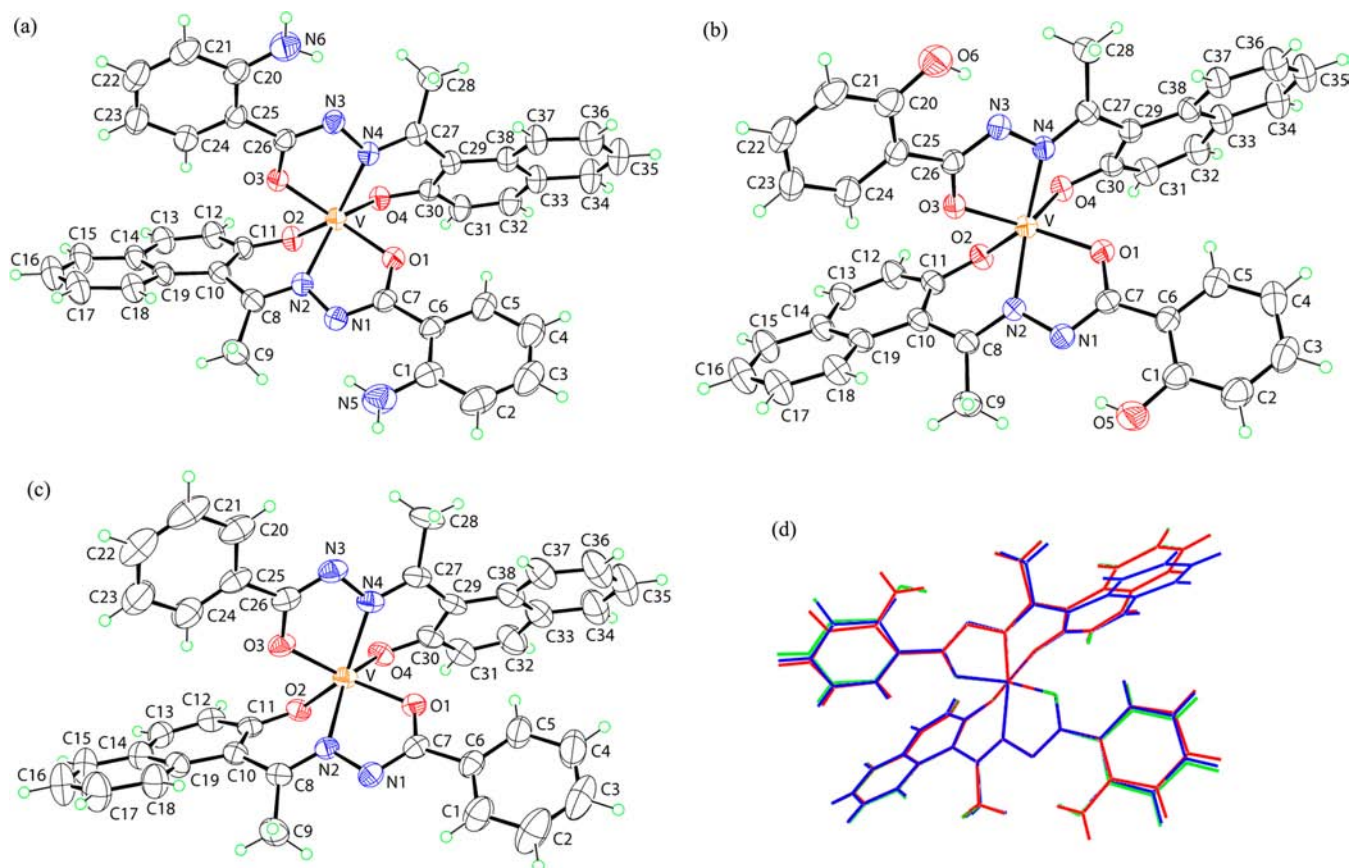
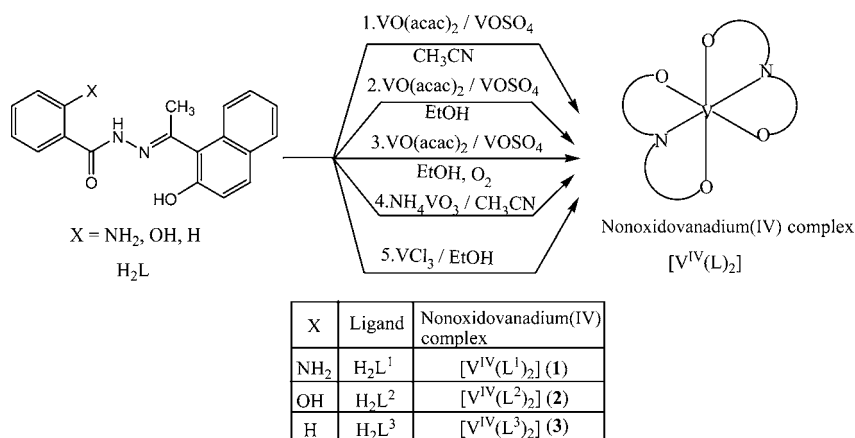


Figure 1. Molecular structures of 1 (a), 2 (b), 3 (c) and overlay diagram of 1 (red image), 2 (green) and 3 (blue) drawn so that the V, O1 and O2 atoms are coincident (d).

[V^{IV}(L²)₂] (2). Yield: 65%. Anal. Calcd. for C₃₈H₂₈N₄O₆V: C, 66.37; H, 4.10; N, 8.15. Found: C, 66.40; H, 4.07; N, 8.17. IR (KBr pellet, cm⁻¹): 3427 ν (O–H); 1591 ν (C=N); 1250 ν (C–O)_{enolic}; 1047 ν (N–N). ESI-MS (CH₂Cl₂): m/z 710.10 (50%, [M + Na]⁺); ESI-MS (CH₃CN + CH₂Cl₂) (19:1): m/z 710.10 (100%, [M + Na]⁺); ESI-MS (MeOH + DMF) (19:1): m/z 710.20 (100%, [M + Na]⁺).

[V^{IV}(L³)₂] (3). Yield: 68%. Anal. Calcd. for C₃₈H₂₈N₄O₄V: C, 69.62; H, 4.30; N, 8.54. Found: C, 69.58; H, 4.31; N, 8.57. IR (KBr pellet, cm⁻¹): 1598 ν (C=N); 1243 ν (C–O)_{enolic}; 1046 ν (N–N). ESI-MS (CH₂Cl₂): m/z 655.25 (90.27%, [M]⁺); ESI-

MS (CH₃CN + CH₂Cl₂) (19:1): m/z 678.27 (100%, [M + Na]⁺); ESI-MS (MeOH + DMF) (19:1): m/z 678.25 (100%, [M + Na]⁺).

Alternatively, these complexes can also be synthesized from the starting materials, like VCl₃, VOSO₄, and NH₄VO₃, as shown in Scheme 1. The spectral data matched well with the values reported above.

X-ray Crystallography. For all three complexes (1–3), the black crystals were obtained from the reaction mixture. Single crystal X-ray diffraction measurements were performed on a Bruker SMART CCD diffractometer employing graphite-

Table 1. Crystal Data and Refinement Details for 1–3

parameter	1	2	3
formula	C ₃₈ H ₃₀ N ₆ O ₄ V	C ₃₈ H ₂₈ N ₄ O ₆ V	C ₃₈ H ₂₈ N ₄ O ₄ V
formula weight	685.62	687.58	655.58
crystal habit, color	rectangle, red	block, red	hexagon, dark green
cryst size, mm	0.06 × 0.07 × 0.17	0.07 × 0.11 × 0.13	0.05 × 0.16 × 0.26
cryst syst	monoclinic	monoclinic	monoclinic
space group	<i>P</i> 2 ₁ / <i>n</i>	<i>P</i> 2 ₁ / <i>n</i>	<i>P</i> 2 ₁ / <i>c</i>
<i>a</i> , Å	14.608(6)	14.711(4)	13.807(7)
<i>b</i> , Å	14.846(6)	14.697(4)	23.851(12)
<i>c</i> , Å	14.976(6)	15.068(4)	10.249(5)
β , °	97.704(8)	96.590(4)	106.571(10)
<i>V</i> , Å ³	3219(2)	3236.3(15)	3235(3)
<i>Z</i>	4	4	4
density, g/cm ³ (calculated)	1.415	1.411	1.346
μ , cm ⁻¹	0.361	0.362	0.354
reflns collected	36 356	35 724	26 859
independent reflns	7362	7419	7320
reflns with $I \geq 2\sigma(I)$	3686	3887	2745
<i>R</i> (observed data)	0.062	0.071	0.074
<i>a</i> in wghting scheme	0.058	0.065	0.064
<i>R</i> _w (all data)	0.158	0.174	0.196
largest diff. peak and hole e Å ⁻³	0.33 and -0.28	0.34 and -0.28	0.30 and -0.38
CCDC deposition number	928 538	928 539	928 540

monochromated Mo *K* α radiation ($\lambda = 0.71073$) so that $\theta_{\max} = 27.5^\circ$. Data collection and reduction were by standard methods,³⁹ and absorption corrections were applied based on multiple scans.⁴⁰ The structures were solved by direct methods⁴¹ and refined by full-matrix least-squares on F^2 .⁴¹ All non-hydrogen atoms were refined anisotropically, C-bound hydrogen atoms were included in the riding model approximation, and O–H and N–H H atoms were refined with the distance constraint 0.82 ± 0.01 and 0.86 ± 0.01 Å, respectively. In the final cycles of each refinement, a weighting scheme of the form $w = 1/[\sigma^2(F_o^2) + aP^2]$, where $P = (F_o^2 + 2F_c^2)/3$, was introduced. The final difference maps were featureless. Molecular structure diagrams presented in Figure 1 were drawn with ORTEP-3 for Windows^{42a} at the 50% probability level, the overlay diagram in Figure 1d was drawn with QMol,^{42b} while remaining crystallographic diagrams were drawn with DIAMOND.^{42c} A summary of crystal data and refinement details for 1–3 is provided in Table 1.

Crystallographic data in CIF format for the structures have been deposited in the Cambridge Crystallographic Data Centre; CCDC 928 538 for 1, CCDC 928 539 for 2, and CCDC 928 540 for 3. This data can be obtained free of charge via <http://www.ccdc.cam.ac.uk/conts/retrieving.html>, or from the Cambridge Crystallographic Data Centre, 12 Union Road, Cambridge CB2 1EZ, UK; fax: (+44) 1223–336–033; or e-mail: deposit@ccdc.cam.ac.uk.

In Vitro Insulin Mimetic Activity. L6 myoblasts were cultured in DMEM containing 10% FBS, penicillin (100 U/ml), and streptomycin (100 μ g/mL) in a humidified 5% CO₂ incubator at 37°C. To differentiate myotubes, the myoblast cells (5×10^4) were seeded in 24-well plates in DMEM containing 2% FBS. The myoblast cells (5×10^4) were grown for 11 days in 0.4 mL of 2% FBS/DMEM to allow the formation of myotubes. The medium was changed every 2 days. On the 11th day, the cells were washed and incubated in Krebs' bicarbonate buffer (KRBB) for 2 h. Myotubes were then further cultured in KRBB containing 25 mM glucose along with 1, 2,

and 4 μ M of vanadium complexes (1–3) and VO(acac)₃ for 4 h. The insulin (2 μ M) was taken as positive control.⁴³ The residual glucose in the buffer aliquots remaining in each well after 4 h was estimated using the hexokiase method by Randox autoanalyzer.

Cytotoxic Assay. Human HeLa cervical cells were obtained from the National Centre of Cell Science (NCCS), Pune, India, and were maintained in minimal essential medium supplemented with 10% fetal bovine serum, penicillin–streptomycin solution and incubated at 37 °C in 5% CO₂ and 95% humidified incubator. HeLa cells were harvested from maintenance cultures in logarithmic phase, after counting in a hemocytometer using trypan blue solution. The cell concentration was adjusted to 5×10^4 cells/ml, and the cells were plated in a 96-well flat bottom culture plate and incubated for 72 h with various concentrations of the test complexes, which were dissolved in a 90% (v/v) DMF solution. The effect of the drugs on the cancer cell viability was studied using the MTT dye reduction assay by measuring the optical density at 595 nm using a microplate reader spectrophotometer (Perkin-Elmer 2030).⁴⁴ The DMF solutions that were used to dissolve the drugs were also used in the control group treatment.

Nuclear Staining. Nuclear staining using the DAPI stain was performed according to the method previously described.⁴⁵ Briefly, HeLa cells either treated or untreated with test compounds were smeared on a clean glass slide, cells were fixed with 3.7% formaldehyde for 15 min, permeabilized with 0.1% Triton X-100, and stained with 1 μ g/mL DAPI for 5 min at 37 °C. The cells were then washed with PBS and examined by fluorescence microscopy (Olympus IX 71) to ascertain any condensation or fragmentation of the nuclei, indicating cells undergoing apoptosis.

■ RESULT AND DISCUSSION

Synthesis. Scheme 1 presents the various pathways through which the nonoxido vanadium(IV) hexacoordinated [V^{IV}(L)₂]₂ complexes were obtained. Reactions of aroylhydrazones

(H₂L¹⁻³) with [VO(acac)₂] or VOSO₄ in acetonitrile or ethanol lead to the formation of monomeric bis(tridentate)–vanadium(IV) complexes [V^{IV}(L¹⁻³)₂] (1–3). The reactions are clean, affording large quantities of pure crystalline products in good yield (~70%). These compounds are highly soluble in CH₂Cl₂, DMF, and DMSO and sparingly soluble in MeOH, EtOH, and CH₃CN.

Alternatively, these nonoxido V^{IV} complexes can also be isolated directly by the reaction of aroylhydrazones with various oxidovanadium(V) and vanadium(III) compounds as starting materials. The formation of [V^{IV}(L)₂] complexes from oxidovanadium(V), NH₄VO₃, and vanadium(III), VCl₃, species probably involves a one-step reduction from vanadium(V) to vanadium(IV), and a one step oxidation from vanadium(III) to vanadium(IV) in open air, respectively, followed by oxido abstraction from the oxidovanadium(IV) species generated in situ. It is noteworthy that the entire synthetic route above can be carried out in laboratory grade ethanol or acetonitrile under ambient conditions. The reactions do not require dry solvent, the presence of base, or an inert atmosphere, which is unusual compared to previous reports.^{29c,e,o,x,46}

Complexes 1–3 are highly stable both in the solid state and in solution. For example, a solution of 1 in different coordinating or noncoordinating solvents does not give any oxidized product (no color change, no oxido-V^{IV}, no oxido-V^V, as confirmed by ESI mass, time dependent UV–vis, and EPR spectroscopy) after exposure to aerial oxygen for 3–4 days or even purging oxygen gas into its solution, a rather uncommon observation for nonoxidovanadium(IV) complexes. Again, to check the stability of these nonoxidovanadium(IV) species, all three complexes (1–3) were dissolved and recovered back from solvent mixture (MeOH + DMF) (9:1) after keeping three days in solution. The isolated solid products were characterized by different spectroscopic techniques (Figures S1–S3). The results matched well regardless of having been recorded using the original compound or the isolated compound from solvent. The absence of a vanadium oxo (V=O) peak in the IR spectrum, no disappearance of low energy transition peaks in UV–vis spectrum, and time-dependent EPR clearly discard the formation of corresponding V(V) in solution. The stability of the complexes may be due to the simultaneous removal of the oxido group, complete charge neutralization as well as the formation of six strong covalent bonds at the V⁴⁺ center from the hard donor atoms N and O, which possibly precludes the approach of a reagent species within the reaction sphere of the well-protected V⁴⁺ center. Also, the rigidity and steric bulk of the ligands do not permit the formation of the square pyramidal pentacoordinated V^VOL(OR) complex so familiar in vanadium chemistry, in which the terminal oxygen is in an axial position and the tridentate ligand occupies the equatorial plane.

Structure Description. Crystals were obtained for each of 1–3, and their crystal structures were determined. Molecular structures are illustrated in Figure 1, and selected geometric parameters are collected in Table 2. In 1, the central V atom is coordinated by two dinegative, NO₂-coordinating hydrazone ligands forming five-membered CN₂OV and six-membered C₃NOV chelate rings. The five-membered rings have envelope conformations with the V atom lying 0.215(5) and 0.301(5) Å above the plane of the remaining atoms of the O1 and O3 chelate rings (rms deviation = 0.0061 Å for each). Each five-membered ring is virtually coplanar to the attached benzene ring (dihedral angles between least-squares planes = 4.17(16) and 7.04(15)°, respectively), which allows for the formation of

Table 2. Selected Geometric Parameters (Å, °) for 1–3

parameter	1	2	3
coordination geometry			
V–O1	1.903(2)	1.919(2)	1.903(3)
V–O2	1.895(2)	1.902(2)	1.906(3)
V–O3	1.891(2)	1.908(2)	1.894(3)
V–O4	1.878(2)	1.888(2)	1.900(3)
V–N2	2.053(3)	2.058(3)	2.073(4)
V–N4	2.066(3)	2.081(3)	2.065(4)
O1–V–O2	126.48(10)	127.59(11)	126.66(13)
O1–V–O3	137.78(10)	136.73(11)	136.77(14)
O1–V–O4	87.33(10)	87.26(10)	87.06(14)
O1–V–N2	74.41(10)	74.75(11)	74.22(15)
O1–V–N4	86.84(10)	87.05(11)	86.86(15)
O2–V–O3	86.27(10)	86.23(10)	87.22(14)
O2–V–O4	84.47(9)	83.75(10)	83.87(13)
O2–V–N2	81.43(10)	81.27(11)	82.11(14)
O2–V–N4	143.32(10)	141.64(11)	142.77(14)
O3–V–O4	125.70(10)	126.99(11)	126.80(14)
O3–V–N2	87.21(10)	86.94(11)	86.92(14)
O3–V–N4	74.47(10)	74.65(11)	74.24(15)
O4–V–N2	143.13(10)	141.72(11)	142.62(14)
O4–V–N4	82.14(10)	81.96(11)	82.14(15)
N2–V–N4	127.22(10)	129.20(11)	127.47(15)
hydrogen bonds			
H...N1	2.03(4)	1.91(4)	
Y...N1	2.710(5) (Y = N5)	2.626(4) (Y = O5)	
H...N3	2.10(4)	1.86(4)	
Y...N3	2.716(4) (Y = N6)	2.628(4) (Y = O6)	
Y–H...N1	135(3) (Y = N5)	147(4) (Y = O5)	
Y–H...N3	128(3) (Y = N6)	153(4) (Y = O6)	

intramolecular N–H...N hydrogen bonds between an amino-H and noncoordinating azo N atoms, Table 2. The six-membered chelate rings exhibit significantly greater deviations from planarity and may to a first approximation be described as having an envelope conformation with the V atom lying well out of the plane (i.e., 0.963(3) Å) defined by the remaining five atoms (rms deviation = 0.0949 Å); the equivalent parameters for the O4 chelate ring are 0.904(3) and 0.1200 Å, respectively. This distortion enables the V atom to exist within a N₂O₄ donor set that approximates a trigonal prism. In this description, the two triangular faces are defined by the (O1, O4, N4) and (O2, O3, N2) atoms. The dihedral angle between the trigonal faces is 2.67(9)°, and the twist of one face relative to the other is 13.5° (cf., 0° for an ideal trigonal prism and 60° for an ideal octahedron). The structure of 2 is isostructural with 1 and presents very similar coordination geometry.

For the two five-membered rings in 2, the V atom lies 0.196(5) and 0.270(5) Å above the plane defined by the remaining four atoms (rms deviation = 0.0033 and 0.0061 Å for the O1 and O3 rings, respectively). The adjacent benzene ring is approximately coplanar to the respective five-membered ring forming dihedral angles of 1.81(17) and 4.88(17)°; this arrangement enables intramolecular O–H...N hydrogen bonding, Table 2. Significant distortions are again evident for the six-membered chelate rings with the V atom lying 0.960(4) Å out of the plane through the remaining five atoms of the O2 chelate ring (rms deviation = 0.0943 Å); the equivalent values for the O4 chelate are 0.926(4) and 0.1181 Å, respectively. In

terms of coordination geometry, the dihedral angle between the trigonal faces is $2.00(10)^\circ$, and the twist angle is 10.1° . While not isostructural with **1** and **2**, the structure of **3** presents all the hallmarks just described with the exception of the intramolecular hydrogen bonding.

For the five-membered rings in **3**, the V atom lies $0.215(6)$ and $0.252(7)$ Å out of the planes of the O1 (rms deviation = 0.0087 Å) and O3 chelate (0.0139 Å) rings, confirming the flattened envelope conformations. Despite the lack of an intramolecular hydrogen bond, as for **1** and **2**, the adjacent five- and six-membered chelate and benzene rings are coplanar forming dihedral angles of $4.9(3)$ and $10.4(3)^\circ$. For the six-membered chelate rings, the V atom lies $0.975(4)$ Å out of the plane of the remaining atoms (rms deviation = 0.1064 Å) for the O2 chelate ring— $0.981(5)$ and 0.1064 Å for the O4 chelate ring. Finally, the dihedral angle between the trigonal face is $2.85(12)^\circ$, and the twist angle is 10.0° .

The overlap diagram, Figure 1d, where the V, O1, O2 atoms have been superimposed, highlights the similarity in the molecular structures of **1–3**, there being only minor differences in the orientations of the peripheral substituents. This homogeneity is reflected in the geometric parameters collated in Table 2, with no significant differences apparent in the bond lengths about the three V atoms. In the same way, no trends are discerned from the bond angles, indicating that the amino (**1**) and hydroxyl (**2**) groups do not exert an influence on the molecular structure even though they form intramolecular hydrogen bonds with the noncoordinating azo N atoms.

In the crystal structure of **1**, no specific intermolecular contacts were identified as being significant employing the distance criteria established in PLATON,⁴⁷ implying the second amino-H atom does not form a significant intermolecular contact. As shown in Figure S4, molecules are arranged in rows along the *b*-axis and are surrounded by molecules forming hydrophobic contacts. In isostructural **2**, a similar packing is observed, but in this case a C–H... π , edge-to-face interaction is formed between methyl-H and the C1-benzene ring of centrosymmetrically related molecules to form dimeric aggregates (for details see Figure S5). As for **1**, no specific intermolecular interactions are noted in the crystal structure of **3** (Figure S6). A macroscopic difference in the global crystal packing is apparent as molecules in **3** can be described as aggregating in the *bc*-plane with the flat layers stacking along the *a*-axis. By contrast, molecules in each of **1** and **2** aggregate in a zigzag pattern parallel to the *ab*-plane and stack along the *c*-axis.

IR Spectroscopy. The IR data of all the ligands (H_2L^{1-3}) and their corresponding metal complexes (**1–3**) are given in the Experimental Section. All the ligands possess a band in the region of $3542\text{--}3337\text{ cm}^{-1}$ due to aromatic –OH present in the naphthalene moiety, which is absent in the corresponding metal complexes due to the coordination. However, the presence of a band at 3427 cm^{-1} in the case of complex **2** is due to the –OH group attached to the benzene nucleus of the ligand H_2L^2 . Disappearance of bands for –NH and –C=O and appearance of bands in the range of $1256\text{--}1243\text{ cm}^{-1}$ indicates the enolization of these two groups forming a –N=C–O– type of bond. Absence of $\nu(\text{V}=\text{O})$ bands in the range of $1035\text{--}935\text{ cm}^{-1}$ clearly indicate the nonoxido nature of the complex.⁴⁸

UV Spectroscopy. Electronic spectra of the complexes **1–3** were recorded in CH_2Cl_2 , DMF, and different mixture solvents like $\text{H}_2\text{O} + \text{DMF}$ (19:1) and $\text{MeOH} + \text{DMF}$ (19:1). In all solutions, the spectral features are quite similar for all three

complexes (Figures S7–S10). The spectral data from CH_2Cl_2 are summarized in Table 3, and the representative spectrum is

Table 3. Electronic Spectra for **1–3 in CH_2Cl_2**

complex	wavelength (nm) (ϵ_{max} ($\text{M}^{-1}\text{cm}^{-1}$))
$[\text{V}^{\text{IV}}(\text{L}^1)_2]$, 1	633 (16174), 509 (13278), 368 (52404), 325 (65737), 265 (80382), 229 (99234)
$[\text{V}^{\text{IV}}(\text{L}^2)_2]$, 2	619 (13060), 507 (13770), 388 (48743), 312 (54808), 253 (89508), 229 (109781)
$[\text{V}^{\text{IV}}(\text{L}^3)_2]$, 3	614 (10273), 501 (9508), 361 (29726), 319 (46775), 265 (56666), 229 (72568)

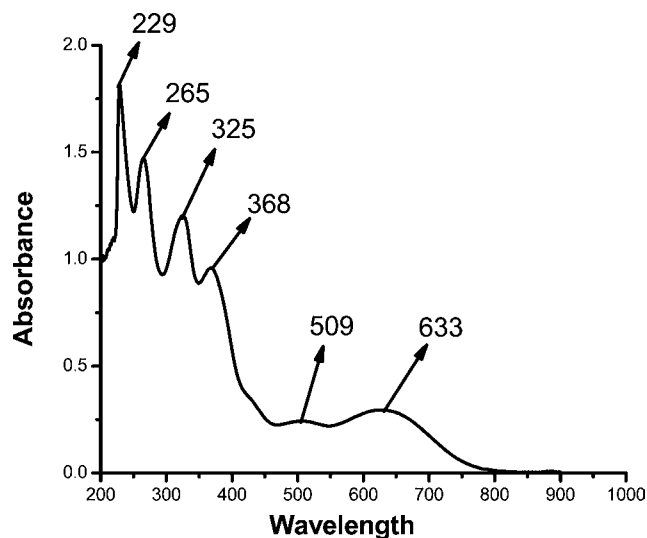


Figure 2. UV-vis spectra of **1** (1.83×10^{-5} M) in CH_2Cl_2 .

shown in Figure 2. There are two bands in the 633–501 nm range, among which, the lowest-energy transition band around 633–614 nm is situated in the d–d transition region, but the intensity (ϵ_{max} , $16174\text{--}10273\text{ M}^{-1}\text{cm}^{-1}$) of this band appears too large for a pure d–d transition, for which the intensity is generally very low for vanadium(IV) complexes. The high intensity of these two bands (633–501 nm) and analogy with other “bare” vanadium(IV) complexes^{29a–c,e,j,h,o,p,x} suggest that these transitions are most reasonably assigned as ligand-to-metal charge transfer in origin. The other bands in the higher energy absorptions (388–229 nm) are likely to be due to ligand centered transitions.^{36b} In **1** and **2**, the bands are slightly red-shifted relative to **3**, presumably a consequence of the electron-releasing –NH₂ and –OH substituent on the ligands in **1** and **2**, respectively.²⁹ⁿ

NMR Spectroscopy. ¹H and ¹³C NMR of the ligands (H_2L^{1-3}) are recorded in DMSO-*d*₆, and the data are given in the Experimental Section. The spectra of the free ligands (H_2L^{1-3}) exhibit a resonance in the range of $\delta = 10.35\text{--}10.21$ ppm due to naphthyl –OH, $\delta = 10.37\text{--}9.17$ ppm due to –NH, and $\delta = 2.35\text{--}2.32$ ppm due to –CH₃ protons, respectively. All the aromatic protons of the ligands are clearly observed in the expected region, $\delta = 7.94\text{--}6.23$ ppm.^{36a,b}

From the ¹³C NMR spectra, it is observed that signals for (CO–N) and (N=C(Me)) carbon resonate in the downfield region in the range of $\delta = 161.19\text{--}153.71$ ppm and $\delta = 155.89\text{--}152.47$ ppm, respectively, whereas the carbon due to the methyl groups (–CH₃) are found in the upfield region ($\delta =$

24.30–24.09 ppm). Furthermore appearance of signals in the range of $\delta = 152.50$ – 113.59 ppm due to aromatic carbon confirm the formation of the ligands.⁴⁹

ESI Mass Spectroscopy. ESI mass spectra of the complexes 1–3 have been recorded in dichloromethane solution. Mass spectral analysis for 3 shows the characteristic molecular ion peak (M^+) at m/z 655.25, whereas for compounds 1 and 2, ESI-MS peaks are observed at m/z 708.49 $[(M + Na)^+]$ and 710.10 $[(M + Na)^+]$, respectively. The ESI mass spectra have also been recorded from different solvent mixtures like $CH_3CN + CH_2Cl_2$ (19:1) and $MeOH + DMF$ (19:1). The results matched well regardless of having been recorded in solutions with coordinating or noncoordinating solvents (Figures S11–S12). The ESI mass data are summarized in the Experimental Section.

Electrochemical Properties. The electrochemical properties of 1–3 have been examined in CH_2Cl_2 solution (0.1 M TEAP) by cyclic voltammetry using a Pt working electrode, Pt auxiliary electrode, and an Ag/AgCl reference electrode. The voltammogram pattern is similar for 1–3, which includes both an oxidation and a reduction process corresponding to one electron transfer. The potential data are listed in Table 4, and

Table 4. Cyclic Voltammetric Results for 1–3 at 298 K^a

complex	$E_{1/2}^a$ (V)	ΔE_p^a (mV)	$E_{1/2}^c$ (V)	ΔE_p^c (mV)
$[V^{IV}(L^1)_2]$, 1	1.10	300	– 0.54	240
$[V^{IV}(L^2)_2]$, 2	1.11	340	– 0.55	270
$[V^{IV}(L^3)_2]$, 3	1.09	280	– 0.53	220

^aIn CH_2Cl_2 at a scan rate of 100 mV s^{-1} . $E_{1/2} = (E_{pa} + E_{pc})/2$, where E_{pa} and E_{pc} are anodic and cathodic peak potentials vs Ag/AgCl, respectively. $\Delta E_p = E_{pa} - E_{pc}$.

Figure 3 depicts a representative voltammogram of 3. In the anodic region, complexes show a quasi-reversible single electron wave (Figure 3a) at $E_{1/2}$ values within the potential window of 1.11 to 1.09 V, which is assigned to the oxidation of the metal, $V(IV)/V(V)$.⁵⁰ In the cathodic region, $V(IV)$ is reduced to $V(III)$, which shows a quasi-reversible single electron wave (Figure 3b) at $E_{1/2}$ values within the potential window of -0.55 to -0.53 V .⁵¹

Magnetic Properties. Magnetic susceptibility data for 1–3 were collected over the temperature range of 2–300 K in an applied magnetic field of 1 T, and a representative temperature dependence of the magnetic susceptibility is shown in Figure S13. At 300 K, 1–3 have effective magnetic moments (μ_{eff}) of 1.64, 1.66, and $1.68 \mu_B$, respectively. These results are typical

for a compound with spin 1/2 per formula unit, suggesting that complexes are monomeric with no or very weak antiferromagnetic interaction between V atoms (intermolecular coupling).^{52,53}

EPR Spectroscopy. X-band EPR spectra of 1–3 were recorded in CH_2Cl_2 solution in the frozen state (77 K). The data are listed in Table 5. A representative frozen solution spectrum for 3 is shown in Figure 4, which reveals well-resolved axial anisotropy with 8-line hyperfine structure, characteristic of a mononuclear vanadium complex with nuclear spin (^{51}V , $I = 7/2$).⁵⁴ Corresponding spin-Hamiltonian parameters (g_{\parallel} , 1.948–1.945; A_{\parallel} , $129.43 \times 10^{-4} \text{ cm}^{-1}$ – $126.94 \times 10^{-4} \text{ cm}^{-1}$; g_{\perp} , 1.996–1.983; A_{\perp} , $42.4 \times 10^{-4} \text{ cm}^{-1}$ – $40.8 \times 10^{-4} \text{ cm}^{-1}$) are typical of trigonal prismatic oxidovanadium(IV) complexes under comparable ON-containing donor environments.^{29a,o} Analysis of the EPR spectra of vanadium(IV) complexes showed that the anisotropic hyperfine parameters of six-coordinate complexes^{35g,54} have significantly lower values compared to the corresponding values obtained with the five-coordinated complexes,^{35e,f,36a,55} as is observed in the present case. The EPR spectra have also been recorded from DMF solution, and the results matches well with the original spectrum reported above (Figure S14).

In Vitro Insulin Mimetic Activity. Vanadium compounds are known to have an insulin mimetic effect.⁵⁶ In this study, 1–3 were tested for their insulin mimetic potential in an in vitro glucose uptake assay. In L6 myotubes, a cell line of skeletal muscle origin, glucose uptake in response to insulin stimulation plays a key role in whole body glucose homeostasis. Glucose transporter (GLUT) 4 is the major glucose transporter of muscle exquisitely regulated by insulin through post-translational events.⁵⁷ The L6 myotubes differentiated from the L6 myoblast have the ability to respond to insulin via insulin receptor signaling and translocation of Glut 4 to the plasma membrane. The hyperglycemic condition was created in cell culture by incubating the cells in 25 mM glucose. In the present experiment, 3 at $4 \mu\text{M}$ had a glucose uptake comparable to $2 \mu\text{M}$ insulin, taken as the positive control (Figure 5). The other two complexes (1 and 2) have moderate insulin mimetic activity, and $VO(\text{acac})_2$ showed negligible activity at the concentrations tested. In the case of 3, the enhancement of the insulin mimetic activity, with respect to 1 and 2, might be related to their different structural characteristics, specifically, the lack of hydrogen bonding functionality in 3. As 3 showed glucose uptake stimulating activity in the myotubes comparable to that of insulin, it is likely that 3 mimics insulin action via

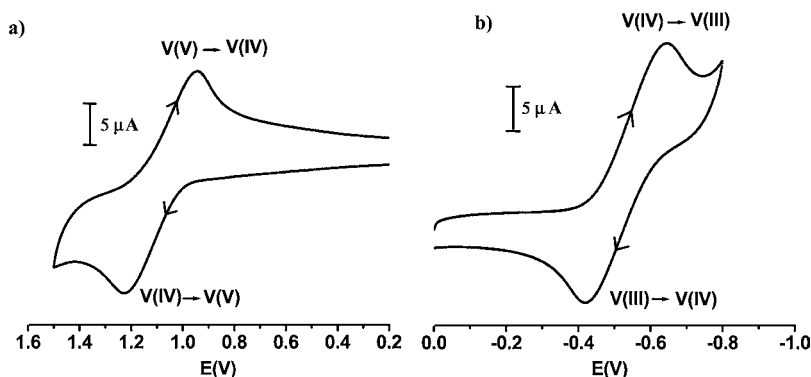


Figure 3. Cyclic voltammogram of 3 showing (a) oxidation ($V(IV) \rightarrow V(V)$) and (b) reduction ($V(IV) \rightarrow V(III)$) of the vanadium(IV) center.

Table 5. X-Band EPR Data for Complexes 1–3 at 77 K^a

complex	g_{\parallel}	g_{\perp}	g_{av}	$A_{\parallel}(10^{-4} \text{ cm}^{-1})$	$A_{\perp}(10^{-4} \text{ cm}^{-1})$	$A_{av}(10^{-4} \text{ cm}^{-1})$
$[\text{V}^{\text{IV}}(\text{L}^1)_2]$, 1	1.947	1.983	1.971	128.25	41.8	70.61
$[\text{V}^{\text{IV}}(\text{L}^2)_2]$, 2	1.945	1.991	1.975	129.43	42.4	71.41
$[\text{V}^{\text{IV}}(\text{L}^3)_2]$, 3	1.948	1.996	1.980	126.94	40.8	69.51

$$^a g_{av} = \frac{1}{3} (2 g_{\perp} + g_{\parallel}). A_{av} = \frac{1}{3} (2A_{\perp} + A_{\parallel}).$$

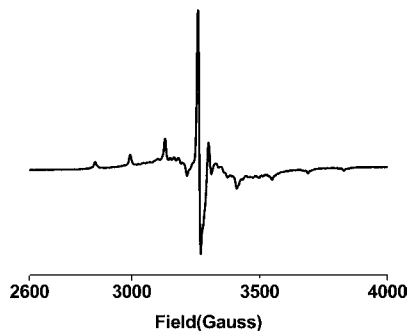


Figure 4. Frozen solution X-band EPR spectrum (77 K) in CH_2Cl_2 of complex 3. Instrument settings: power, -0.009 dB; modulation, 100 kHz; sweep center, 2500 G; sweep time, 120 s; sweep width, 2500 G.

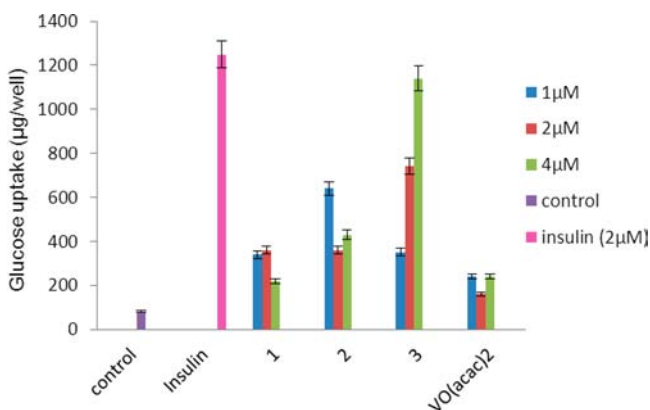


Figure 5. Effect of vanadium complexes (1–3) on glucose uptake in cultured L6 myotubes under high glucose conditions (25 mM Glucose). Three concentrations (1 μM , 2 μM and 4 μM) were tested for each complex. The data are indicated as mean \pm SEM ($n = 3$). Student's t -test was used where bars with asterisk show a significant difference ($*P < 0.05$) with respect to the untreated control.

insulin receptor signaling with translocation of Glut 4 to the plasma membrane.

Inhibition of Cancer Cell Viability. In the present study, antiproliferative efficacy of 1–3 was assayed by determining the viability of HeLa cells using the MTT assay. The ligands H_2L^{1-3} and $\text{VO}(\text{acac})_2$ gave high IC_{50} values of $>200 \mu\text{M}$, whereas 1–3 gave values in the range of 41–22 μM . In contrast, cisplatin, gefitinib, gemcitabine, 5-fluorouracil, and vinorelbine, the most commonly used chemotherapeutic drugs, are comparably effective in HeLa cells with an IC_{50} value of 13, 20, 35, 40, and 48 μM , respectively, under similar experimental conditions.⁵⁸ The significant decrease in the inhibitory concentration for the ligand compared to the metal complex clearly indicates that incorporation of vanadium in the ligand environment has a marked effect on cytotoxicity. A possible explanation is that by coordination, the polarity of the ligand and the central metal ion are reduced through the charge equilibration, which favors permeation of the complexes

through the lipid layer of the cell membrane.^{59,60} The present results are consistent with the observation that metal complexes can exhibit greater biological activities than the free ligand.^{20a}

Comparing the activity of three complexes, the cytotoxicity follows the order of $2 > 3 > 1$, which is reflected from their IC_{50} values with dose dependency illustrated in Figure 6. It is remarkable that 2, containing the ortho-hydroxy group, is most active suggesting that the electron-withdrawing and releasing nature of the ortho-substituent may exert an influence over antiproliferative activity. Specifically, 2 was most cytotoxic, a result correlated with the presence of the electron-withdrawing hydroxyl group. On the other hand, the presence of an electron-donating substituent ($-\text{NH}_2$) in the ligand core of 1 diminishes cytotoxicity, which is reflected in its IC_{50} value. For complex 3, the value is between because of not having an electron-withdrawing or a releasing group in the ligand. Very recently, the antiproliferative activity of some oxidovanadium(IV) compounds has been reported by Yamaguchi et al. using the similar technique against U937 cells, and the present results are in accordance with the reported values.⁶¹

Nuclear Staining Assay. To investigate the apoptotic potential of test compounds in HeLa cells, DAPI staining was performed. Chromatin condensation during the process of apoptosis (type I programmed cell death) is a characterizing marker of nuclear alteration. HeLa cells were treated with 25, 20, and 35 μM of 1, 2, and 3, respectively, that is, at doses less than their respective IC_{50} values. The cells were incubated for 24 h before DAPI nuclear staining. Cells were examined under fluorescent microscope fitted with a DAPI filter. Control cells (treated with 90% DMF) hardly showed any sort of condensation in comparison to the treated cells (see Figure 7). All images taken in grayscale demonstrate the brightly condensed chromatin bodies and the nuclear blebbings, as marked by arrows in Figure 7. Besides showing nuclear change, the treated cells exhibited a shrinking morphology, which is another important hallmark of apoptosis.

CONCLUSION

The following are the salient observations and findings of this work: (a) Three aroylhydrazone ligands, possessing a rigid, bulky 2-hydroxy-1-acetonaphthone core and a selection of anthranil-, salicyl- and benzoyl-hydrazide arms have been synthesized and utilized in the synthesis of the corresponding vanadium complexes. As expected, monomeric, hexacoordinated and bis(tridentate)-vanadium(IV) $[\text{V}^{\text{IV}}(\text{L})_2]$ complexes were isolated; these do not contain an oxido-group. Stability of the complexes are related to the simultaneous oxido removal and complete charge neutralization as well as the formation of six strong covalent bonds at the V^{4+} center from the hard donor atoms N and O. (b) The importance of the structural and electronic effects arising from the incorporation of a bulky 2-hydroxy-1-acetonaphthone group in the ketone part of aroylhydrazones that can stabilize six-coordinate nonoxidovanadium(IV) complexes has been highlighted, which can be compared with our earlier work on

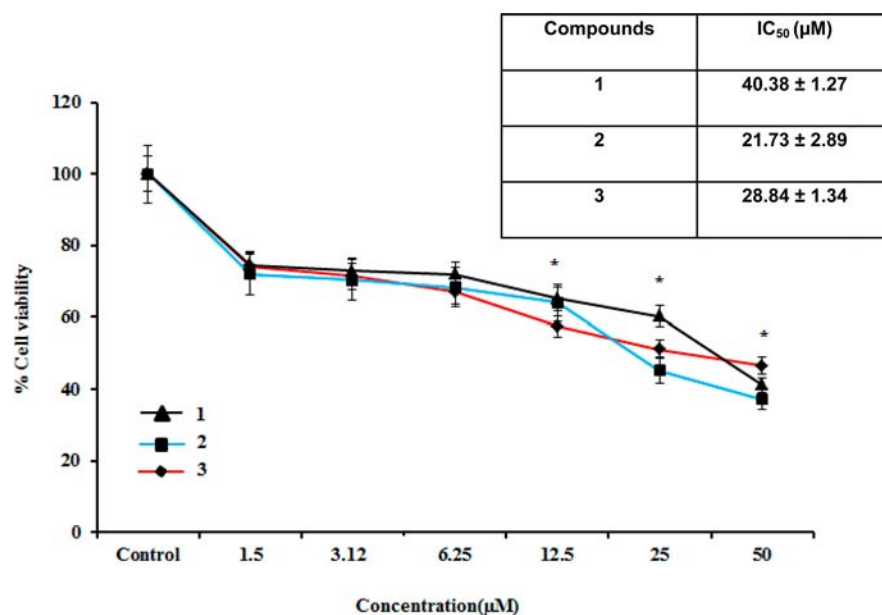


Figure 6. Effect of 1, 2, and 3 on cell viability and growth: HeLa cells were treated with different concentrations of the test compound for 72h, and then cell viability was measured by MTT assay. Data reported as the mean \pm SD for $n = 6$ and compared against PBS control by using a Student's t -test. (*significant compared to PBS control).

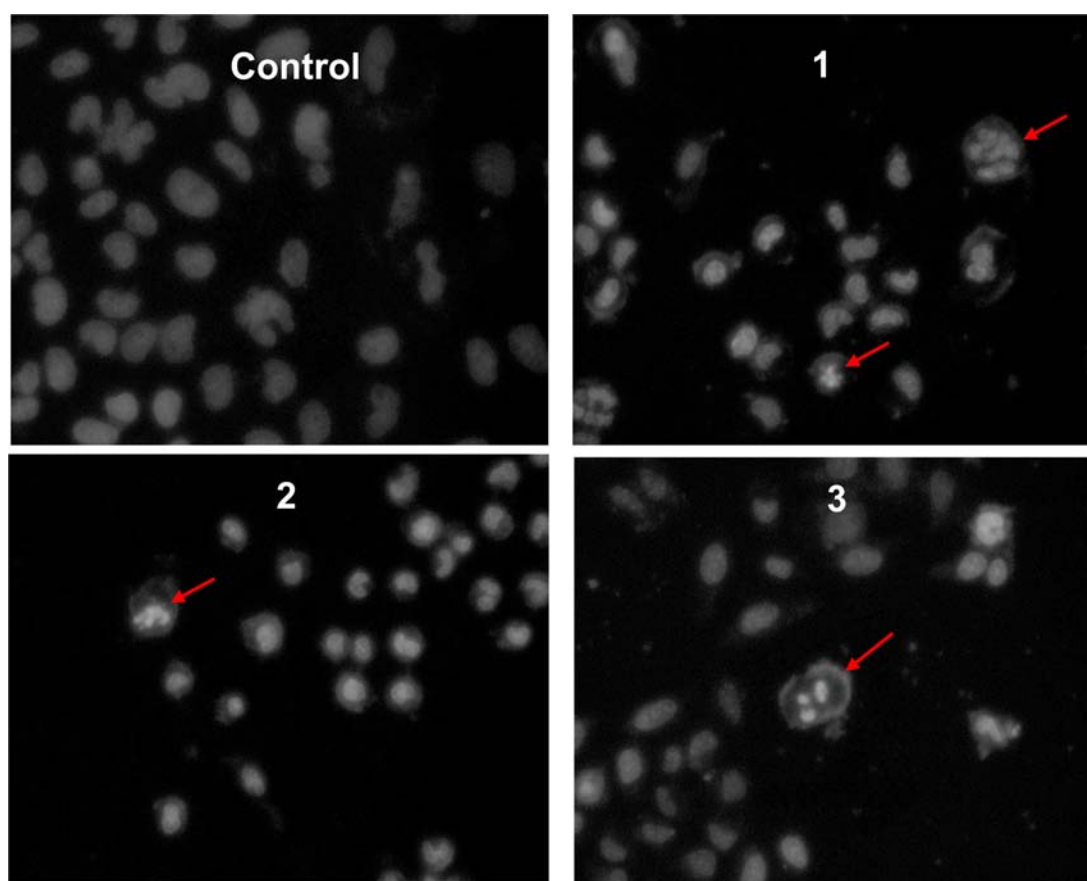


Figure 7. Study of apoptosis by morphological changes in nuclei of HeLa cells: After treatment, HeLa cells from the control and treatment group were fixed with 3.7% formaldehyde for 15 min, permeabilized with 0.1% Triton X-100, and stained with 1 μ g/mL DAPI for 5 min at 37 °C. The cells were then washed with PBS and examined by fluorescence microscopy (Olympus IX 71) (200 \times). Arrows show the morphological changes in the nuclei of HeLa cells observed on applying drug (1–3) in comparison to control.

oxidovanadium(V) with ligand-containing ONO donor atoms.^{36a,b} (c) Complexes 1–3 are highly stable both in the solid

state and in solution, being resistant to exposure to aerial oxygen for 3–4 days and even purging oxygen into their

solutions, a rather unusual phenomenon for “bare” vanadium(IV) or nonoxidovanadium(IV) complexes. (d) EPR and magnetic susceptibility data provide reference values for typical V(IV) sites. Electrochemical results suggest that the electrochemical oxidations and reductions are not ligand-centered but metal-centered, generating V^V and V^{III} species, respectively. (e) All the complexes show in vitro insulin mimetic activity against insulin responsive L6 myoblast cells, with complex 3 being the most potent, which is comparable to insulin at the complex concentration of 4 μ M, while the others have moderate insulin mimetic activity. In addition, the in vitro antiproliferative activity of complexes 1–3 against the HeLa cell line was assayed. The cytotoxicity of the complexes is affected by the various functional groups attached to the bezoylhydrazone derivative, and 2 showed considerable antiproliferative activity. It is worth noting that although the structure and chemistry of few nonoxidovanadium(IV) hydrazone complexes has been recently described,^{29a,p} the suitability of these and the related nonoxidovanadium(IV) complexes in the study of vanadium insulin mimesis and antiproliferative activity has not been previously described.

■ ASSOCIATED CONTENT

■ Supporting Information

IR spectra of complex 1 and isolated compound 1' (Figure S1), UV–vis spectra of compound 2' in CH_2Cl_2 as solvent (Figure S2), ESI mass spectra of isolated compound 1' [A] in ($CH_3CN + CH_2Cl_2$ (19:1); [B] in (MeOH + DMF) (19:1) (Figure S3), view in projection down the *b*-axis of the unit cell contents of 1 (Figure S4), view in projection down the *b*-axis of the unit cell contents of 2 (Figure S5), view in projection down the *c*-axis of the unit cell contents of 3 (Figure S6), time-dependent UV–vis spectra of complex 2 in DMF as solvent (Figure S7), time-dependent UV–vis spectra of complex 3 in DMF as solvent (Figure S8), time-dependent UV–vis spectra of complex 2 in solvent mixture ($H_2O + DMF$) (19:1) (Figure S9), time-dependent UV–vis spectra of complex 3 in solvent mixture (MeOH + DMF) (19:1) (Figure S10), ESI mass spectra of complex 3 ($CH_3CN + CH_2Cl_2$) (19:1) (Figure S11), ESI mass spectra of complex 3 (MeOH + DMF) (19:1) (Figure S12), temperature dependence of the magnetic susceptibility of complex 3 (Figure S13), time-dependent frozen solution X-band EPR spectrum (77 K) of complex 3 in DMF at 0.5 h interval. (Figure S14). This material is available free of charge via the Internet at <http://pubs.acs.org>.

■ AUTHOR INFORMATION

Corresponding Author

*E-mail: rupamdinda@nitrrkl.ac.in.

Author Contributions

The manuscript was written through contributions of all authors. All authors have given approval to the final version of the manuscript.

Notes

The authors declare no competing financial interest.

■ ACKNOWLEDGMENTS

The authors thank the reviewers for their comments and suggestions, which were helpful in preparing the revised version of the manuscript. Funding for this research was provided by Department of Science and Technology, Government of India (Grants SR/FT/CS-016/2008 and SR/WOS-A/CS-145/

2011). R. D. thanks Prof. M. Chaudhury and Prof. M. R. Maurya for fruitful discussion and Prof. S. K. Chattopadhyay for discussion and electrochemical study. R. D. also thanks Dr. T. K. Maji for the magneto chemistry and Dr. T. K. Paine, and Dr. P. Sen for EPR analysis. The Ministry of Higher Education (Malaysia) and the University of Malaya (UM) is thanked for funding crystal engineering studies through the High-Impact Research scheme (UM.C/HIR-MOHE/SC/03).

■ REFERENCES

- (1) (a) Rehder, D. *Coord. Chem. Rev.* **1999**, *182*, 297. (b) Rehder, D. *J. Inorg. Biochem.* **2000**, *80*, 133–136.
- (2) Nriagu, J. O. *Adv. Environ. Sci. Technol.* **1998**, *30*, 1–24.
- (3) (a) Meisch, H. U.; Bielig, H. J. *Basic Res. Cardiol.* **1980**, *75*, 413. (b) Baran, E. J. *Adv. Plant Physiol.* **2008**, *10*, 357–372. (c) Anke, M. *Anales de la Real Academia Nacional de Farmacia* **2004**, *70*, 961–999.
- (4) (a) Cantley, L. C., Jr; Josephson, L.; Warner, R.; Yanagisawa, M.; Lechene, C.; Guidotti, G. *J. Biol. Chem.* **1977**, *252*, 7421–7423. (b) Morsy, M. D.; Abdel-Razek, H. A.; Osman, O. M. *J. Physiol. Biochem.* **2011**, *67*, 61–69.
- (5) (a) Rehder, D.; Santonin, G.; Licini, G. M.; Schulzke, C.; Meier, B. *Coord. Chem. Rev.* **2003**, *237*, 53–63. (b) Plass, W. *Coord. Chem. Rev.* **2003**, *237*, 205–212. (c) Thompson, K. H.; Orvig, C. *Coord. Chem. Rev.* **2001**, *219*, 1033–1053. (d) Butler, A. *Coord. Chem. Rev.* **1999**, *187*, 17–35.
- (6) (a) Frausto da Silva, J. J. R.; Williams, R. J. P. *The Biological Chemistry of the Elements*, 2nd ed.; Oxford University Press: Oxford, U.K., 2001. (b) Kaim, W.; Schwederski, B. *Bioinorganic Chemistry: Inorganic Elements in the Chemistry of Life*; John Wiley & Sons: Chichester, U. K., 1994. (c) Eady, R. R. *Coord. Chem. Rev.* **2003**, *237*, 23–30.
- (7) (a) Wei, Y.; Zhang, C.; Zhao, P.; Yang, X.; Wang, K. *J. Inorg. Biochem.* **2011**, *105*, 1081–1085. (b) Rehder, D.; Costa Pessoa, J.; Geraldes, C. F. G. C.; Kabanos, T.; Kiss, T.; Meier, B.; Micera, G.; Pettersson, L.; Rangel, M.; Salifoglou, A.; Turel, I.; Wang, D. *J. Biol. Inorg. Chem.* **2002**, *7*, 384–396. (c) Sutradhar, M.; Barman, T. R.; Mukherjee, G.; Kar, M.; Saha, S. S.; Drew, M. G. B.; Ghosh, S. *Inorg. Chim. Acta* **2011**, *368*, 13–20. (d) Saltiel, A. R.; Khan, C. R. *Nature* **2001**, *414*, 799–806. (e) Noblíá, P.; Baran, E. J.; Otero, L.; Gambino, D. *Eur. J. Inorg. Chem.* **2004**, 322–328. (f) Nilsson, J.; Shteinman, A. A.; Rehder, D.; Nordlander, E. *J. Inorg. Biochem.* **2011**, *105*, 1795–1800. (g) Willsky, G. R.; Chi, L.-H.; Hu, Z.; Crans, D. C. *Coord. Chem. Rev.* **2011**, *255*, 2258–2269. (h) Rehder, D. *Inorg. Chem. Commun.* **2003**, *6*, 604–617. (i) Islam, M. N.; Kumbhar, A. A.; Kumbhar, A. S.; Joshi, B. N. *Inorg. Chem.* **2010**, *49*, 8237–8246. (j) Pillai, S. I.; Subramanian, S. P.; Kandaswamy, M. *Eur. J. Med. Chem.* **2013**, *63*, 109–117.
- (8) (a) Shechter, Y.; Karlsh, S. J. D. *Nature* **1980**, *284*, 556–558. (b) Heyliger, C. E.; Tahiliani, A. G.; McNeill, J. H. *Science* **1985**, *227*, 1474–1477.
- (9) Ramanadham, S.; Mongold, J. J.; Brownsey, R. W.; Cros, G. H.; McNeill, J. H. *Am. J. Physiol.* **1989**, *257*, H904–H911.
- (10) McNeill, J. H.; Yuen, V. G.; Hoveyda, H. R.; Orvig, C. *J. Med. Chem.* **1992**, *35*, 1489–1491.
- (11) Schecter, Y.; Meyerovitch, J.; Farfel, Z.; Sack, J.; Bar-Meir, S.; Amir, S.; Degani, H.; Karlsh, S. J. D. *Vanadium in Biological Systems*; Kluwer Academic Publishers: Norwell, MA, 1990; p 129.
- (12) Thompson, K. H.; McNeill, J. H.; Orvig, C. *Topics in Biological Chemistry: Metallopharmaceuticals*; Springer-Verlag: Heidelberg, 1999; Vol. 2, pp 139–158.
- (13) (a) Sakurai, H.; Fugono, J.; Yasui, H. *Mini-Rev. Med. Chem.* **2004**, *4*, 41–48. (b) Adachi, Y.; Yoshida, J.; Kodera, Y.; Katoh, A.; Takada, J.; Sakurai, H. *J. Med. Chem.* **2006**, *49*, 3251–3256. (c) Melchior, M.; Thompson, K. H.; Jong, J. M.; Rettig, S. J.; Shuter, Ed; Yuen, V. G.; Zhou, Y.; McNeill, J. H.; Orvig, C. *Inorg. Chem.* **1999**, *38*, 2288–2293. (d) Yamaguchi, M.; Wakasugi, K.; Saito, R.; Adachi, Y.; Yoshikawa, Y.; Sakurai, H.; Katoh, A. *J. Inorg. Biochem.* **2006**, *100*, 260–269. (e) Crans, D. C.; Mahroof-Tahir, M.; Johnson,

- M. D.; Wilkins, P. C.; Yang, L.; Robbins, K.; Johnson, A.; Alfano, J. A.; Godzala, M. E., III; Austin, L. T.; Willsky, G. R. *Inorg. Chim. Acta* **2003**, 356, 365–378. (f) Karmaker, S.; Saha, T. K.; Yoshikawa, Y.; Yasui, H.; Sakurai, H. J. *Inorg. Biochem.* **2006**, 100, 1535–1546.
- (14) Thompson, K. H.; Liboiron, B. D.; Sun, Y.; Bellman, K. D. D.; Setyawati, I. A.; Patrick, B. O.; Karunaratne, V.; Rawji, G.; Wheeler, J.; Sutton, K.; Bhanot, S.; Cassidy, C.; McNeill, J. H.; Yuen, V. G.; Orvig, C. *J. Biol. Inorg. Chem.* **2003**, 8, 66–74.
- (15) Rosenberg, B.; Camp, L. V.; Trosko, J. E.; Mansour, V. H. *Nature* **1969**, 222, 385–386.
- (16) Orvig, C.; Abrams, M. J. *Chem. Rev.* **1999**, 99, 2201–2203.
- (17) Kovala-Demertzi, D.; Bocciarelli, A.; Demertzis, M. A.; Coluccia, M. *Chemotherapy* **2007**, 53, 148–152.
- (18) Sakurai, H.; Kojima, Y.; Yoshikawa, Y.; Kawabe, K.; Yasui, H. *Coord. Chem. Rev.* **2002**, 226, 187–198.
- (19) Louie, A. Y.; Meade, T. J. *Chem. Rev.* **1999**, 99, 2711–2734.
- (20) (a) Rosu, T.; Pahontu, E.; Pasculescu, S.; Georgescu, R.; Stanica, N.; Curaj, A.; Popescu, A.; Leabu, M. *Eur. J. Med. Chem.* **2010**, 45, 1627–1634. (b) Padhye, S.; Afrasiabi, Z.; Sinn, E.; Fok, J.; Mehta, K.; Rath, N. *Inorg. Chem.* **2005**, 44, 1154–1156. (c) Ali, A. A.; Nimir, H.; Aktas, C.; Huch, V.; Rauch, U.; Schäfer, K. H.; Veith, M. *Organometallics* **2012**, 31, 2256–2262.
- (21) Kovala-Demertzi, D.; Papageorgiou, A.; Papathanasis, L.; Alexandratos, A.; Dalezis, P.; Miller, J. R.; Demertzis, M. A. *Eur. J. Med. Chem.* **2009**, 44, 1296–1302.
- (22) Rebolledo, A. P.; Vieites, M.; Gambino, D.; Piro, O. E.; Castellano, E. E.; Zani, C. L.; Souza-Fagundes, E. M.; Teixeira, L. R.; Batista, A. A.; Beraldo, H. J. *Inorg. Biochem.* **2005**, 99, 698–706.
- (23) Djordjevic, C. *Metal Ions Biol. Systems* **1995**, 31, 595–616.
- (24) Sakurai, H.; Tamura, H.; Okatani, K. *Biochem. Biophys. Res. Commun.* **1995**, 206, 133–137.
- (25) Dong, Y.; Narla, R. K.; Sudbeck, E.; Uckun, F. M. *J. Inorg. Biochem.* **2000**, 78, 321–330.
- (26) Noleto, G. R.; Petkowicz, C. L. O.; Mercê, A. L. R.; Nosedá, M. D.; Méndez-Sánchez, S. C.; Reicher, F.; Oliveira, M. B. M. *J. Inorg. Biochem.* **2009**, 103, 749–757.
- (27) Sasmal, P. K.; Saha, S.; Majumdar, R.; Dighe, R. R.; Chakravarty, A. R. *Inorg. Chem.* **2010**, 49, 849–859.
- (28) (a) Gillard, R. D.; McCleverty, J. A. In *Comprehensive Coordination Chemistry*, Wilkinson, G., Ed.; Pergamon Press, Oxford, England, 1987; Vol. 3, p 453. (b) Cotton, F. A.; Wilkinson, G. *Advanced Inorganic Chemistry*, 5th ed; John Wiley & Sons: New York, 1988; p 665.
- (29) (a) Diamantis, A. A.; Snow, M. R.; Vanzo, J. A. *Chem. Commun.* **1976**, 264–265. (b) Comba, P.; Engelhardt, L. M.; Harrowfield, J. M.; Lawrance, G. A.; Martin, L. L.; Sargeson, A. M.; White, A. H. *Chem. Commun.* **1985**, 174–176. (c) Cooper, S. R.; Koh, Y. B.; Raymond, K. N. *J. Am. Chem. Soc.* **1982**, 104, 5092–5102. (d) Diamantis, A. A.; Manikas, M.; Salam, M.; Snow, M. R.; Tiekink, E. R. T. *Aust. J. Chem.* **1988**, 41, 453–468. (e) Auerbach, U.; Della Vedova, B. P. C.; Wieghardt, K.; Nuber, B.; Weiss, J. *Chem. Commun.* **1990**, 1004–1006. (f) Kang, B.; Wenig, L.; Liu, H.; Wu, D.; Huang, L.; Lu, C.; Cai, J.; Chen, X.; Lu, J. *Inorg. Chem.* **1990**, 29, 4873–4877. (g) Kabanos, T. A.; White, A. J. P.; Williams, D. J.; Woolins, J. D. *Chem. Commun.* **1992**, 17–18. (h) Kabanos, T. A.; Slawin, A. M. Z.; Williams, D. J.; Woolins, J. D. *Dalton Trans.* **1992**, 1423–1427. (i) Bruni, S.; Caneschi, A.; Cariati, F.; Delfs, C.; Dei, A.; Gatteschi, D. *J. Am. Chem. Soc.* **1994**, 116, 1388–1394. (j) Neves, A.; Ceccato, A. S.; Vencato, I.; Mascarenhas, Y. P.; Erasmus-Buhr, C. *Chem. Commun.* **1992**, 652–654. (k) Vergopoulos, V.; Jantzen, S.; Rodewald, D.; Rehder, D. *Chem. Commun.* **1995**, 377–378. (l) Ludwig, E.; Hefele, H.; Uhlemann, E.; Weller, F.; Kläui, W. Z. *Anorg. Allg. Chem.* **1995**, 621, 23–28. (m) Hefele, H.; Ludwig, E.; Uhlemann, E.; Weller, F. Z. *Anorg. Allg. Chem.* **1995**, 621, 1973–1976. (n) Klich, P. R.; Daniher, A. T.; Challen, P. R.; McConville, D. B.; Youngs, W. J. *Inorg. Chem.* **1996**, 35, 347–356. (o) Paine, T. K.; Weyhermüller, T.; Slep, L. D.; Neese, F.; Bill, E.; Bothe, E.; Wieghardt, K.; Chaudhuri, P. *Inorg. Chem.* **2004**, 43, 7324–7338. (p) Sutradhar, M.; Mukherjee, G.; Drew, M. G. B.; Ghosh, S. *Inorg. Chem.* **2007**, 46, 5069–5075. (q) Farahbakhsh, M.; Schmidt, H.; Rehder, D. *Chem. Commun.* **1998**, 2009–2010. (r) Kajiwarra, T.; Wagner, R.; Bill, E.; Weyhermüller, T.; Chaudhuri, P. *Dalton Trans.* **2011**, 40, 12719–12726. (s) Sanna, D.; Várnagy, K.; Lihi, N.; Micera, G.; Garribba, E. *Inorg. Chem.* **2013**, 52, 8202–8213. (t) Stiefel, E. I.; Dori, Z.; Gray, H. B. *J. Am. Chem. Soc.* **1967**, 89, 3353–3354. (u) Raymond, K. N.; Isied, S. S.; Brown, L. D.; Fronczek, F. R.; Nibert, J. H. *J. Am. Chem. Soc.* **1976**, 98, 1767–1774. (v) Karpishin, T. B.; Stack, T. D. P.; Raymond, K. N. *J. Am. Chem. Soc.* **1993**, 115, 182–192. (w) Kondo, M.; Minakoshi, S.; Iwata, K.; Shimizu, T.; Matsuzaka, H.; Kamigata, N.; Kitagawa, S. *Chem. Lett.* **1996**, 25, 489–490. (x) Paine, T. K.; Weyhermüller, T.; Bill, E.; Bothe, E.; Chaudhuri, P. *Eur. J. Inorg. Chem.* **2003**, 4299–4307. (y) Morgenstern, B.; Steinhäuser, S.; Hegetschweiler, K.; Garribba, E.; Micera, G.; Sanna, D.; Nagy, L. *Inorg. Chem.* **2004**, 43, 3116–3126. (z) Morgenstern, B.; Kutzky, B.; Neis, C.; Stucky, S.; Hegetschweiler, K.; Garribba, E.; Micera, G. *Inorg. Chem.* **2007**, 46, 3903–3915.
- (30) (a) Bayer, E.; Kneifel, H. Z. *Naturforsch., B: Chem. Sci.* **1972**, 27, 207. (b) Kneifel, H.; Bayer, E. *J. Am. Chem. Soc.* **1986**, 108, 3075–3077.
- (31) Berry, R. E.; Armstrong, E. M.; Beddoes, R. L.; Collison, D.; Ertok, S. N.; Helliwell, M.; Garner, C. D. *Angew. Chem., Int. Ed.* **1999**, 38, 795–797.
- (32) Terra, L. H. A.; Areias, M. C.; Gaubeur, I.; Suez-Iha, M. E. V. *Spectrosc. Lett.* **1999**, 32, 257–271.
- (33) (a) Maurya, M. R.; Agarwal, S.; Abid, M.; Azam, A.; Bader, C.; Ebel, M.; Rehder, D. *Dalton Trans.* **2006**, 937–947. (b) Savini, L.; Chiasserini, L.; Travagli, V.; Pellerano, C.; Novellino, E. *Eur. J. Med. Chem.* **2004**, 39, 113–122. (c) Cui, Z.; Yang, X.; Shi, Y.; Uzawa, H.; Cui, J.; Dohi, H.; Nishida, Y. *Bioorg. Med. Chem. Lett.* **2011**, 21, 7193–7196.
- (34) (a) Cunha, A. C.; Figueiredo, J. M.; Tributino, J. L. M.; Miranda, A. L. P.; Castro, H. C.; Zingali, R. B.; Fraga, C. A. M.; Souza, M. C. B. V.; Ferreira, V. F.; Barreiro, E. *J. Biorg. Med. Chem.* **2003**, 11, 2051–2059. (b) Easmon, J.; Puerstinger, G.; Thies, K.-S.; Heinisch, G.; Hofmann, J. *J. Med. Chem.* **2006**, 49, 6343–6350. (c) Chaston, T. B.; Watts, R. N.; Yuan, J.; Richardson, D. R. *Clin. Cancer Res.* **2004**, 10, 7365–7374. (d) Braslawsky, G. R.; Edson, M. A.; Pearce, W.; Kaneko, T.; Greenfield, R. S. *Cancer Res.* **1990**, 50, 6608–6614. (e) Darnell, G.; Richardson, D. R. *Blood* **1999**, 94, 781–792. (f) Fan, C. D.; Su, H.; Zhao, J.; Zhao, B. X.; Zhang, S. L.; Miao, J. Y. *Eur. J. Med. Chem.* **2010**, 45, 1438–1446. (g) Morgan, L. R.; Jursic, B. S.; Hooper, C. L.; Neumann, D. M.; Thangaraj, K.; LeBlanc, B. *Bioorg. Med. Chem. Lett.* **2002**, 12, 3407–3411. (h) Dandawate, P.; Khan, E.; Padhye, S.; Gaba, H.; Sinha, S.; Deshpande, J.; Venkateswara, S. K.; Khetmalas, M.; Ahmad, A.; Sarkar, F. H. *Bioorg. Med. Chem. Lett.* **2012**, 22, 3104–3108. (i) Liu, W. Y.; Li, H. Y.; Zhao, B. X.; Shin, D. S.; Lian, S.; Miao, J. Y. *Carbohydr. Res.* **2009**, 344, 1270–1275. (j) Xia, Y.; Fan, C. D.; Zhao, B. X.; Zhao, J.; Shin, D. S.; Miao, J. Y. *Eur. J. Med. Chem.* **2008**, 43, 2347–2353. (k) Effenberger, K.; Breyer, S.; Schobert, R. *Eur. J. Med. Chem.* **2010**, 45, 1947–1954. (l) Hassan, G. S.; Kadry, H. H.; Abou-Seri, S. M.; Ali, M. M.; Mahmoud, A. E. *Bioorg. Med. Chem.* **2011**, 19, 6808–6817. (m) Tian, F. F.; Li, J. H.; Jiang, F. L.; Han, X. L.; Xiang, C.; Ge, Y. S.; Li, L. L.; Liu, Y. *RSC Advances* **2012**, 2, 501–513. (n) Richardson, D. R. *Antimicrob. Agents Chemother.* **1997**, 41, 2061–2063.
- (35) (a) Bhattacharyya, S.; Mukhopadhyay, S.; Samanta, S.; Weakley, T. J. R.; Chaudhuri, M. *Inorg. Chem.* **2002**, 41, 2433–2440. (b) Sutradhar, M.; Mukherjee, G.; Drew, M. G. B.; Ghosh, S. *Inorg. Chem.* **2006**, 45, 5150–5161. (c) Dai, J.; Wang, H. *Polyhedron* **1996**, 15, 1801–1806. (d) Maurya, R. C.; Rajput, S. *J. Mol. Struct.* **2007**, 833, 133–144. (e) Mangalam, N. A.; Sivakumar, S.; Sheeja, S. R.; Kurup, M. R. P.; Tiekink, E. R. T. *Inorg. Chim. Acta* **2009**, 362, 4191–4197. (f) Maurya, R. C.; Rajput, S. *J. Mol. Struct.* **2006**, 794, 24–34. (g) Lu, L.; Yue, J.; Yuan, C.; Zhu, M.; Han, H.; Liu, Z.; Guo, M. *J. Inorg. Biochem.* **2011**, 105, 1323–1328. (h) Sarkar, S.; Aydogdu, Y.; Dagdelen, F.; Bhaumik, B. B.; Dey, K. *Mater. Chem. Phys.* **2004**, 88, 357–363. (i) Kuriakose, M.; Kurup, M. R. P.; Suresh, E. *Polyhedron* **2007**, 26, 2713–2718. (j) Rahchamani, J.; Behzad, M.; Bezaatpour, A.; Jahed, V.; Dutkiewicz, G.; Kubicki, M.; Salehi, M. *Polyhedron* **2011**, 30,

- 2611–2618. (k) Tsuchimoto, M.; Kasahara, R.; Nakajima, K.; Kojima, M.; Ohba, S. *Polyhedron* **1999**, *18*, 3035–3039. (l) Teixeira, M. F. S.; Dockal, E. R.; Cavalheiro, É. T. G. *Sens. Actuators B* **2005**, *106*, 619–625. (m) Maurya, R. C.; Rajput, S. *Prog. Cryst. Growth Charact. Mater.* **2006**, *52*, 142–149. (n) Li, L.; Guo, Z.; Zhang, Q.; Xu, T.; Wang, D. *Inorg. Chem. Commun.* **2010**, *13*, 1166–1169. (o) Grivani, G.; Bruno, G.; Rudbari, H. A.; Khalaji, A. D.; Pourteimouri, P. *Inorg. Chem. Commun.* **2012**, *18*, 15–20. (p) Maurya, M. R.; Sikarwar, S.; Kumar, M. *Catal. Commun.* **2007**, *8*, 2017–2024. (q) El-Taras, A. A.; EL-Mehasseb, I. M.; Ramadan, A. M. C. R. *Chimie* **2012**, *15*, 298–310. (r) Wang, D.; Ebel, M.; Schulzke, C.; Grüning, C.; Hazari, S. K. S.; Rehder, D. *Eur. J. Inorg. Chem.* **2001**, 935–942. (s) Maurya, M. R.; Khan, A. A.; Azam, A.; Kumar, A.; Ranjan, S.; Mondal, N.; Pessoa, J. C. *Eur. J. Inorg. Chem.* **2009**, 5377–5390. (t) Teixeira, M. F. S.; Marcolino-Júnior, L. H.; Fatibello-Filhob, O.; Dockal, E. R.; Cavalheiro, É. T. G. *J. Braz. Chem. Soc.* **2004**, *15*, 803–808. (u) Alyea, E. C.; Dee, T. D.; Ferguson, G. J. *Crystallogr. Spectro. Res.* **1985**, *15*, 29–38. (v) Xu, T.; Li, L. Z.; Zhou, S. F.; Guo, G. Q.; Niu, M. J. *J. Chem. Crystallogr.* **2005**, *35*, 263–267. (w) Salavati-Niasari, M.; Ganjali, M. R.; Norouzi, P. *J. Porous Mater.* **2007**, *14*, 423–432.
- (36) (a) Dinda, R.; Sengupta, P.; Ghosh, S.; Mak, T. C. W. *Inorg. Chem.* **2002**, *41*, 1684–1688. (b) Dinda, R.; Sengupta, P.; Sutradhar, M.; Mak, T. C. W.; Ghosh, S. *Inorg. Chem.* **2008**, *47*, 5634–5640. (c) Dash, S. P.; Pasayat, S.; Bhakat, S.; Dash, H. R.; Das, S.; Butcher, R. J.; Dinda, R. *Polyhedron* **2012**, *31*, 524–529.
- (37) Rowe, R. A.; Jones, M. M. *Inorg. Synth.* **1957**, *5*, 113–116.
- (38) Naskar, S.; Mishra, D.; Butcher, R. J.; Chattopadhyay, S. K. *Polyhedron* **2007**, *26*, 3703–3714.
- (39) SMART and SAINT; Bruker AXS, Inc.: Madison, WI, 1996.
- (40) Sheldrick, G. M. SADABS; University of Göttingen: Göttingen, Germany, 1996.
- (41) Sheldrick, G. M. *Acta Crystallogr.* **2008**, *A64*, 112–122.
- (42) (a) Farrugia, L. J. *J. Appl. Crystallogr.* **2012**, *45*, 849–854. (b) Gans, J.; Shalloway, D. *J. Molec. Graphics Model.* **2001**, *19*, 557–559. (c) Brandenburg, K. DIAMOND; Crystal Impact GbR: Bonn, Germany, 2006.
- (43) Ha, B. G.; Nagaoka, M.; Yonezawa, T.; Tanabe, R.; Woo, J. T.; Kato, H.; Chung, U.; Yakasaki, K. *J. Nutr. Biochem.* **2012**, *23*, 501–509.
- (44) Bhutia, S. K.; Mallick, S. K.; Stevens, S. M.; Prokai, L.; Vishwanatha, J. K.; Maiti, T. K. *Toxicol. In Vitro* **2008**, *22*, 344–351.
- (45) Bhutia, S. K.; Mallick, S. K.; Maiti, S.; Maiti, T. K. *Chem Biol Interact.* **2008**, *174*, 11–18.
- (46) Branca, M.; Micera, G.; Dessi, A.; Sanna, D.; Raymond, K. N. *Inorg. Chem.* **1990**, *29*, 1586–1589.
- (47) Spek, A. L. *Acta Crystallogr.* **2009**, *D65*, 148–155.
- (48) (a) Selbin, J. *Chem. Rev.* **1965**, *65*, 153–175. (b) Selbin, J. *Coord. Chem. Rev.* **1966**, *1*, 293–314.
- (49) Adão, P.; Pessoa, J. C.; Henriques, R. T.; Kuznetsov, M. L.; Avecilla, F.; Maurya, M. R.; Kumar, U.; Correia, I. *Inorg. Chem.* **2009**, *48*, 3542–3561.
- (50) Chatterjee, P. B.; Bhattacharya, S.; Audhya, A.; Ki-Young, C.; Endo, A.; Chaudhury, M. *Inorg. Chem.* **2008**, *47*, 4891–4902.
- (51) Mandal, D.; Chaudhury, M. *Struct. Chem.* **2007**, *18*, 187–193.
- (52) Nakai, M.; Yano, S. *J. Inorg. Biochem.* **2004**, *98*, 105–112.
- (53) Pessoa, J. C.; Cavaco, I.; Correia, I. *Inorg. Chim. Acta* **1999**, *293*, 1–11.
- (54) Parihar, S.; Pathan, S.; Jadeja, R. N.; Patel, A.; Gupta, V. K. *Inorg. Chem.* **2012**, *51*, 1152–1161.
- (55) Samanta, S.; Ghosh, D.; Mukhopadhyay, S.; Endo, A.; Weakley, T. J. R.; Chaudhury, M. *Inorg. Chem.* **2003**, *42*, 1508–1517.
- (56) Islam, M. N.; Kumbhar, A. A.; Kumbhar, A. S.; Zeller, M.; Butcher, R. J.; Dusane, M. B.; Joshi, B. N. *Inorg. Chem.* **2010**, *49*, 8237–8246.
- (57) Ishiki, M.; Klip, A. *Endocrinology* **2005**, *146*, 5071–5078.
- (58) Ahmed, M.; Jamil, K. *Biol. Med.* **2011**, *3*, 60–71.
- (59) Ramadan, A. M. *J. Inorg. Biochem.* **1997**, *65*, 183–189.
- (60) Avaji, P. G.; Kumar, C. H. V.; Patil, S. A.; Shivananda, K. N.; Nagaraju, C. *Eur. J. Med. Chem.* **2009**, *44*, 3552–3559.